# MODELING OF PHOTOEMISSION AND ELECTRON SPIN POLARIZATION FROM NEA GaAs PHOTOCATHODES*

O. Chubenko, A. Afanasev

The George Washington University, Washington, DC 20052, USA

## Abstract

Many nuclear-physics and particle-physics scientific laboratories, including Thomas Jefferson National Accelerator Facility, Newport News, VA 23606 (Jefferson Lab) which studies parity violation and nucleon spin structure, require polarized electron sources. At present, photoemission from strained GaAs activated to negative electron affinity (NEA) is a main source of polarized electrons. Future experiments at advanced electron colliders will require highly efficient polarized electron beams, which sets new requirements for photocathodes in terms of high quantum efficiency (QE) ($\gg$ 1%) and spin polarization ($\approx$ 85%). Development of such materials includes modeling and design of photocathodes, material growth, fabrication of photocathodes, and photocathode testing. The purpose of the present work is to develop a semi-phenomenological model, which could predict photoemission and electron spin polarization from NEA GaAs photocathodes. Detailed Monte Carlo simulation and modeling of physical processes in photocathodes is important for optimization of their design in order to achieve high QE and reduce depolarization mechanisms. Electron-phonon interactions near the surface and influence of the presence of quantum heterostructures on the diffusion length are studied in depth. Simulation results will be compared to the experimental results obtained at Jefferson Lab and can be used to optimize the photocathode design and material growth, and thus develop high-polarization high-brightness electron source.

# INTRODUCTION

For more than 50 years, photoemission from GaAs and GaAs-based photocathodes has been a main source of polarized electrons for many nuclear-physics and particle-physics facilities. Due to a large direct band gap ($E_g = 1.42eV$) and ability to achieve NEA levels (Fig. 1), GaAs can be used to emit polarized electrons efficiently. The efficiency of photocathodes is described by spin polarization, the degree to which the spin is aligned with a given direction, and QE, the ration of the number of emitted electrons to the number of incident photons.

Band model is used to describe optical transitions between valence and conduction bands (Fig. 2). Near the center of Brillouin zone ($\Gamma$ point) transitions between s-type conduction band state ($l = 0$) and p-type valence band state ($l = 1$) are possible. Since $|l - s| \leq j \leq l + s$, conduction band state is doubly degenerate ($j = 1/2$; $m_j = -1/2, 1/2$). For the valence band we have a four-fold degenerate state ($j = 3/2$;

$m_j = -3/2, -1/2, 1/2, 3/2$), which is separated from a doubly degenerate state ($j = 1/2$; $m_j = -1/2, 1/2$) by an energy distance $\Delta \approx 0.3eV$, spin-orbit splitting.

Taking into account four-hold degeneracy of the $j = 3/2$ state, an effective mass description of the valence band structure is commonly used. It is assumed that the valence band consists of two types of holes, the heavy holes ($m_j = \pm3/2$) and light holes ($m_j = \pm1/2$). So the valence band consists of three bands: heavy hole valence band, light hole valence band, and split-off valence band.
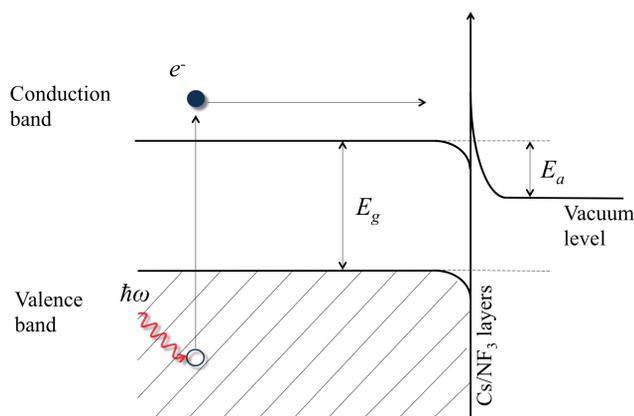


Figure 1: Photoemission from GaAs activated to NEA by putting layers of $Cs$ and $NF_3$ on the surface of photocathode: photoexcitation of valence electrons into the conduction band; transport of electrons to the surface; emission of electrons into the vacuum.

When unstrained GaAs is illuminated by circularly polarized light (right-polarized, for example), two transitions from $P_{3/2}$ state are allowed, with three times as many electrons in one spin state as in the other spin state (Fig. 3). So theoretically, unstrained GaAs can provide maximum 50% polarization. But because of different depolarizing mechanisms, it is limited at about 35%.

To improve polarization, mechanical strain of GaAs crystals is used. GaAs is grown on a thick substrate, for example GaAsP, whose different lattice constant provides the crystal strain resulting in the valence band degeneracy remove. So excitation by the laser light of certain wavelength allows single transitions from the valence band states, theoretically giving 100% polarization (Fig. 4). But again, depolarizing effects decrease this value to 85%.

Alternating layers of strained GaAs form a Super Lattice (SL) structure (Fig. 5), which helps to improve both polarization and QE.
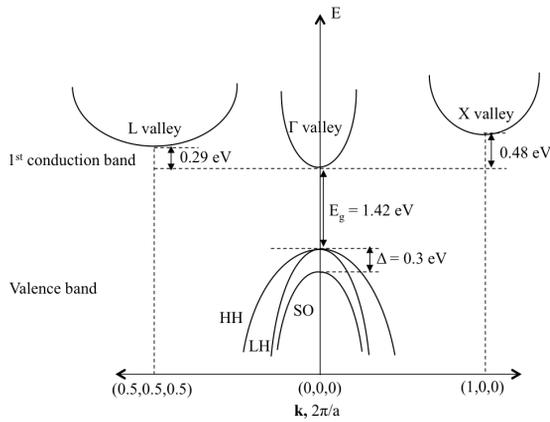
Figure 2: Band structure of GaAs (T = 300 K).
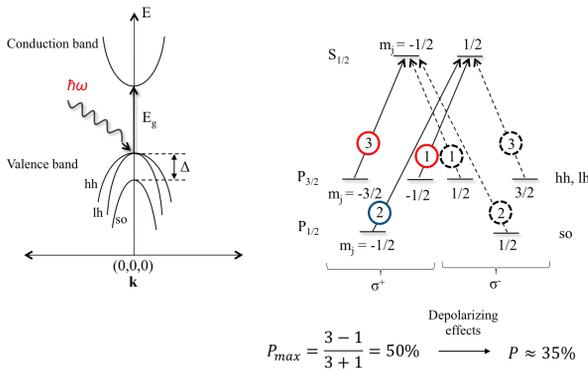


Figure 3: Electromagnetic transition probabilities at the $\Gamma$ point of unstrained GaAs: positive $\sigma^+$ and negative $\sigma^-$ helicities correspond to transitions during excitation by right-polarized (solid lines) and left-polarized (dashed lines) photons, respectively; numbers inside the circles indicate the relative strength of transitions; different colors indicate transitions under excitation by photons of different energy.
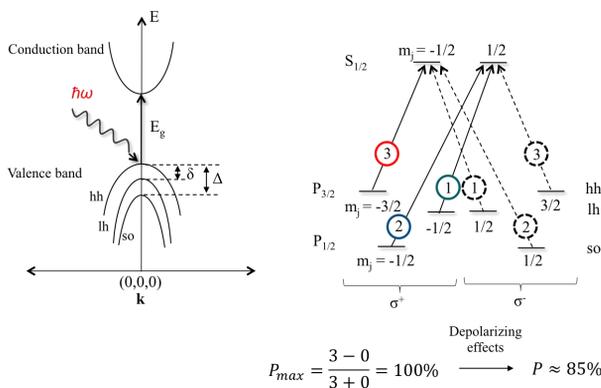


Figure 4: Electromagnetic transition probabilities at the $\Gamma$ point of strained GaAs.

## IMPLEMENTATION OF THE PHOTOEMISSION MODEL

Photoemission from GaAs is effectively described by the three-step model:
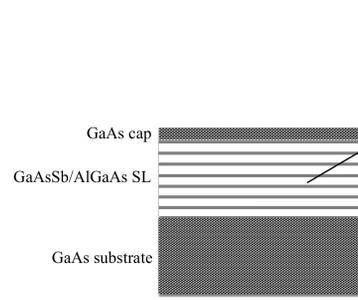


Figure 5: Schematic structure of GaAsSb/AlGaAs SL material.

1. Photoexcitation of valence electrons into the conduction band.
2. Transport of electrons to the surface.
3. Emission of electrons into the vacuum.

Short description of each step is given below.

### Photoexcitation

Light incident on the photocathode surface decays exponentially into the surface. Model developed by Lao and Perera [1] allows to calculate the photon energy dependence of the absorption length for different doping densities using imaginary part of dielectric function.

### Electron Transport

Over the years, detailed Monte Carlo algorithm for direct solution of Boltzmann transport equation has been developed and applied for modeling of electron transport in bulk III-V semiconductors under the influence of applied external field [2], [3]. The present work uses this algorithm to describe transport properties of bulk GaAs. The algorithm will be modified and used to simulate electron transport in presence of heterostructures.

In the simulation, the three-valley model is used to describe the band structure of GaAs. Free carriers interact with the crystal and with each other through different scattering mechanisms that relax energy and momentum of the particle. Scattering mechanisms in semiconductors can be classified into 3 types:

1. Defect Scattering.
2. Carrier-Carrier scattering.
3. Lattice Scattering.

The Monte Carlo algorithm tracks electrons in both real space and $k$-space and takes into account scattering of electrons with acoustic phonons, polar optical phonons, intervalley scattering, and Coulomb scattering. Scattering rates calculated by Fermi's Golden rule for the $\Gamma$ valley are presented in Fig. 6.

The Monte Carlo technique includes generation of random free flight times, random choice of the type of scattering event that occurs at the end of each free flight, and recalculating the energy and momentum of each particle after the scattering. The procedure then repeats for the next free flight and stops after time exceeds maximum simulation time.
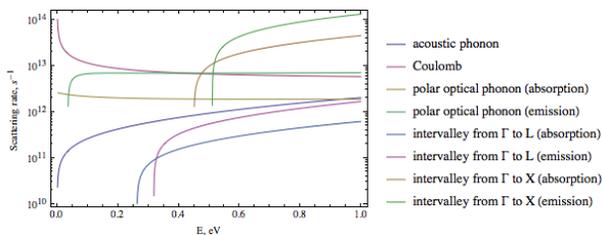
Figure 6: Scattering rates for the $\gamma$ valley.

After the simulation is completed, typical results to check are velocity-time characteristic and field dependence of such characteristics as drift velocity and valley occupancy. The results are presented in Figs. 7- 8, respectively.
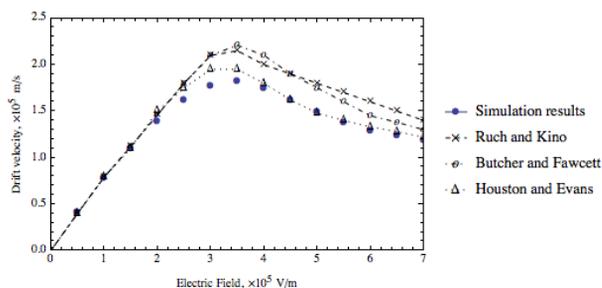


Figure 7: Field dependence of the electron drift velocity compared to experimental results [4]- [6].
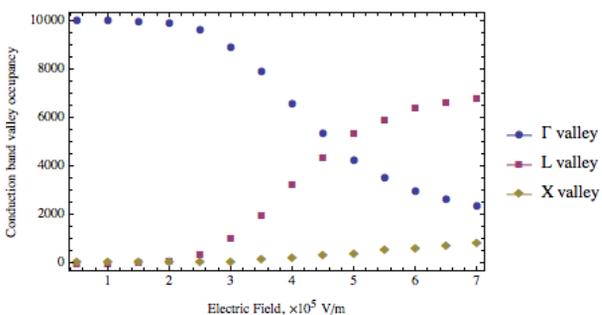


Figure 8: Field dependence of the conduction band valley occupancy.

## Emission

There are four main surface effects, which must be considered in the emission step:

1. Band bending region.
2. Scattering during emission.
3. Surface barrier.

The exact nature or shape of the surface barrier is not very well understood. Two contributors to this barrier are: the double dipole effect due to the $Cs/NF_3$ layer at the surface and the image charge effect. Usually consider rectangular or triangular surface barriers (Fig. 9).

## Presence of Heterostructures

Simulation of electron transport in heterostructures requires some modifications in the Monte Carlo algorithm.
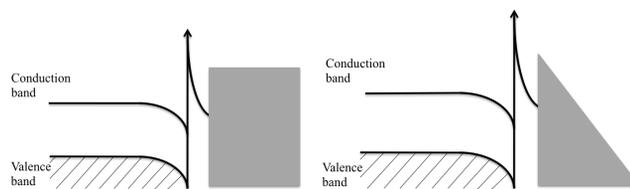


Figure 9: Models of surface barrier.

First of all, scattering from the potential barrier due to the presence of semiconductor with greater band gap needs to be added.
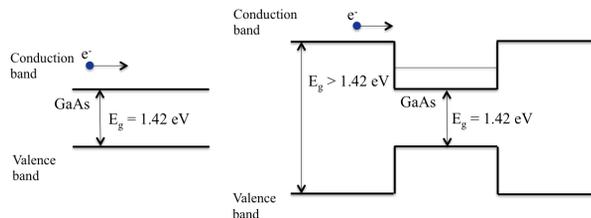


Figure 10: Band structure of bulk GaAs and double heterostructure, created by combining semiconductors with different band gap. If an active region is narrow enough, then quantum confinement occurs.

Another characteristic, which is often used to describe transport properties of semiconductors, is diffusion length $L$, which is defined as

$$L = \sqrt{D\tau}, \qquad (1)$$

where $D$ is the diffusion constant and $\tau$ is the lifetime of the minority carrier. The last one is defined for heterosteuctures as

$$\frac{1}{\tau_H} = \frac{1}{\tau_B} + \frac{2s}{d}, \qquad (2)$$

where $s$ is an average of the front and back interface recombination velocities, $d$ is the thickness of the active layer, and lifetime of minority carrier in bulk material $\tau_B$ is defined by radiative, Shockley-Read-Hall (SRH), and Auger recombination mechanisms

$$\frac{1}{\tau_B} = \frac{1}{\tau_{rad}} + \frac{1}{\tau_{SRH}} + \frac{1}{\tau_{Auger}}. \qquad (3)$$

## CONCLUSION

The present paper describes preliminary results of modeling photoemission from NEA GaAs photocathodes. The model will be developed and applied to GaAs-based photocathodes with heterostructures.

## ACKNOWLEDGMENT

# REFERENCES

[1] Y.-F. Lao and A. G. U. Perera, J. Appl. Phys. 109, 103528 (2011).

[2] D. Vasileska and S. M. Goodnick, "Bulk Monte Carlo: Implementation details and source codes download", `http://nanohub.org/resources/9109`, 2010.

[3] S. Karkare *et al.*, "Monte Carlo charge transport and photoemission from negative electron affinity GaAs photocathodes", J. Appl. Phys., 113, 104904, 2013.

[4] J. G. Ruch and G. S. Kino, Phys. Rev. 174, 921 (1968).

[5] P. Butcher and W. Fawcett, Phys. Letters 21, 489 (1966).

[6] P. A. Houston and A. G. R. Evans, Solid State Electron 20, 197 (1977).